Nanomicelles co-loaded with doxorubicin and salvianolic acid A for breast cancer chemotherapy

Zhiyong Li
School of Pharmacy, Yantai University
Jiali Liu
School of Pharmacy, Yantai University
Zheng Sun
School of Pharmacy, Yantai University
Yanli Li
School of Pharmacy, Yantai University
Bin Yu
School of Pharmacy, Yantai University
Feng Zhao
School of Pharmacy, Yantai University
Hongbo Wang
School of Pharmacy, Yantai University
Hui Xu (xuhui33@sina.com)
School of Pharmacy, Yantai University

Research Article

Keywords: Multifunctional nanomicelles, Doxorubicin, Salvianolic acid A, Breast cancer chemotherapy, Cardioprotection

Posted Date: March 21st, 2022

DOI: https://doi.org/10.21203/rs.3.rs-1355560/v1

Abstract

Background: Multi-drug delivery system based on polymer carrier is emerging for alleviating dose-limiting toxicities of first-line cytotoxic anticancer drugs such as doxorubicin (DOX) for breast cancer chemotherapy. By co-loading the premium natural antioxidant salvianolic acid A (SAA) through colloidal self-assembly of amphiphilic copolymer, we herein developed CPMSD, a complex polymeric micellar system to overcome cardiotoxicity associated with DOX.

Results: Optimal formulation was obtained by DOE study and CPMSD micelles were well constructed by using mPEG-PCL for entrapment at a drug-carrier mass ratio of 1:5 and DOX-SAA mass ratio of 1:4. Molecular dynamics simulation revealed the ratiometrical co-encapsulation of SAA into the hydrophobic cavity but DOX to ball-shaped surface of micelles due to hydrophilicity. Characterization study manifested favorable biopharmaceutical properties such as small and uniform particle size, fairly high drug loading capacity, as well as good colloidal stability and controlled drug release. CPMSD maintained anticancer efficacy of DOX and the action mechanism, which did not be affected by co-administering SAA. More to the point, it was of great benefit to systemic safety and cardio-protective effect against oxidative stress injuries associated with DOX in tumor-bearing mice.

Conclusions: All the findings substantiated that CPMSD would be a promising multifunctional nanosystem of DOX for breast cancer chemotherapy.

Introduction

Breast cancer is among the most frequently diagnosed cancer and now becomes the leading cause of cancer death in women worldwide.[1] According to the latest data from the International Agency for Research on Cancer (IARC) of the World Health Organization (WHO), more than 2.26 million new cases of breast cancer were diagnosed in 2020, which were responsible for 11.7% of all new cases of cancer. So far, chemotherapy remains an essential treatment for preventing recurrence in many patients with stage I-III breast cancer. Given the relatively unfavorable prognosis, it is even the sole systemic therapy with demonstrated efficacy for triple-negative breast cancer (TNBC), and only chemotherapeutic agents are approved by the Food and Drug Administration (FDA).[2]

The anthracycline antibiotic doxorubicin (DOX, Fig. 1) is one of the most effective chemotherapeutic agents approved for various cancers, which is also most commonly used in standard regimens such as AC4, AC-T, and TaxAC for breast cancer. Specifically, the use of DOX appears most important in patients with more lymph node involvement and with TNBC disease.[3] Overall, chemotherapy regimens containing both DOX and taxane achieve the greatest risk reduction and remain the appropriate choice in high-risk patients [1]. However, the clinical application of DOX is usually associated with multiple adverse effects, particularly the cardiac mortality that may affect ~ 11% of the patients under treatment.[4] More to the point, DOX related cardiotoxicity is typically a kind of dose-limiting toxicity, leading to limited cumulative tolerable dose and lowered therapeutic efficacy. It has been demonstrated that even 26% of patients

develop congestive heart failure at a cumulative dose of 550 mg/m^2 of DOX.[5] Therefore, the DOX therapies with attenuated toxicity but maintained anticancer efficacy are still a great challenge.

Over the past decades, much research has been devoted to investigating solution ways against DOX-induced cardiotoxicity, mainly including development of new drug delivery systems and discovery of efficient cardio-protective adjuvants. The pegylated liposomal doxorubicin (Doxil) is a liposome-encapsulated form of DOX available in the market with reduced cardiotoxicity and an improved pharmacokinetic profile. Major limitations of this improved DOX formulation are complicated preparation process and high cost, although several clinical trials have demonstrated that its monotherapy is an effective alternative to other commonly used chemotherapy regimens in patients with metastatic breast cancer.[6] Meanwhile, various cardiac protective agents have been evaluated, including dexrazoxane, the only one approved by FDA for treatment of anthracycline extravasation.[7, 8] Unfortunately, its clinical use has been restricted due to carcinogenic potential with an increased risk for development of acute myeloid leukemia and myelodysplastic syndrome.[9, 10] In recently years, oxidative stress caused by excessive production of reactive oxygen species (ROS) has been the most widely investigated and accepted mechanism of DOX induced cardiotoxicity, and natural antioxidative molecules with good efficacy and safety have attracted increasingly high attention.[11–15] However, drug delivery system research is still a huge challenge to realize further development and clinical application of these promising cardio-protective candidates mainly due to undesirable physico-chemical properties.

Nanofabrication by self-assembly provides polymeric micelles (PMs) a typical core-shell structure, which solubilizes and stabilizes hydrophobic molecule in the core, while the hydrophilic shell can improve the steric stabilization by reducing opsonization and prolong blood circulation.[16–18] With the advantages of adequate function and easy manufacture, PMs are becoming more and more attractive in drug delivery, especially for co-delivering conventional cytotoxic agent and some medical adjuvant to produce distinctive effect of killing two birds with one stone.[19–21] Much recent research has demonstrated that salvianolic acid A (SAA, Fig. 1), an active polyphenol from *Salvia miltiorrhiza*, is a potent natural antioxidant with great benefit against various oxidative stress injuries such as DOX-induced cardiotoxicity. Recently it has been approved in China for oral administration for the treatment of diabetic peripheral neuropathy, and angina attack and acute myocardial infarction, respectively.[22–25] As shown in Fig. 1, the present study just aimed to develop a complex nanomicellar formulation (CPMSD) that dually loaded DOX and SAA to produce multiple beneficial effects for breast cancer chemotherapy. By using bio-compatible copolymer as drug carrier, the novel formulation of CPMSD provided an efficient way co-delivering SAA with DOX for injection, also overcome the major limitations of its unsatisfactory physicochemical properties such as instability, poor solubility and low systemic bioavailability.[26–28] Herein the multifunctional nanomicellar system of CPMSD was fabricated under the optimal formulation to meet the demands of clinical application, and both the therapeutic efficacy and mechanism of action were investigated via *in vitro* and *in vivo* models. To the best of our knowledge, so far there have been no reports about complex nano-formulation co-delivering DOX and SAA. There is no doubt that the resulting

multifunctional nanomicellar system of CPMSD would pay the way for breast cancer chemotherapy with DOX-containing regimens.

Material And Methods

Materials

Doxorubicin hydrochloride (DOX) was supplied by Beijing Ouhe Technology Co., Ltd (Beijing, China), and salvianolid acid A (SAA) was purchased from Nanjing Guangrun Biotechnology Co., Ltd. (Nanjing, China), respectively. The macroinitiator used was polyethylene ethylene glycol monomethyl ether (mPEG) with a number-average molecular weight of 2,000 obtained from Sigma-Aldrich Co (St Louis, MO, USA), and all the amphiphilic diblock copolymers were synthesized in our laboratory by ring-opening polymerization according to the method previously reported[29]. All solvents and other reagents were available commercially and of analytical grade or higher. Ultra-pure water prepared by a lab purification system was used throughout the experiment.

Cells and animals

The MCF-7 human breast adenocarcinoma cell line was acquired from Chinese Academy of Science Cell Bank for Type Culture Collection (Shanghai, China). DMEM containing 10% fetal bovine serum and 1% penicillin/streptomycin (HyClone Laboratories, Logan, USA) was used for cell culture in a humidified incubator with 5% CO_2 at 37°C. The female athymic nude mice (BALB/c, nu/nu) with body weight of 20 ± 2 g (aging from 6 to 8 weeks) were obtained from Shanghai Experimental Animal Center (Shanghai, China). All animal experimental procedures were conducted by following the National Institutes of Health (NIH) guidelines and approved by the Animal Experimentation Ethics Committee of Yantai University, China.

Preparation of CPMSD and characterization

By using amphiphilic diblock copolymer as drug carrier, the nanomicelles co-encapsulating DOX and SAA (CPMSD) were prepared via a simple and reliable thin-film hydration method as previously reported.[21] In brief, a specified amount of co-polymer and SAA were firstly dissolved in acetone at first. After 5 minutes of stirring, the solvent was slowly evaporated under water bath at 45 ± 2°C to form a thin-layer film, dissolved with physiological saline at 45°C to obtain a transparent micelle solution, followed by successive addition of the phosphate-buffered solution (PBS; 10×, pH 7.4) and DOX aqueous solution. The mixture was stirred at room temperature (~ 20 min), filtered through a 0.22-μm filter, then subjected to lyophilization under vacuum (FD-1C-80 freeze-dryer, Shanghai, China) to obtain the freeze-dried powder of CPMSD stored at -20°C until use.

The micelles were reconstituted to obtain an aqueous solution (~ 1 mg/mL) for morphology observation by using transmission electron microscopy (JEM-1400 TEM, JEOL, Tokyo, Japan). The mean diameter and particle size distribution were measured by dynamic light scattering method (Zetasizer Nano ZS 90,

Malvern, UK) at room temperature with a scattering angle of 90°, and the polydispersity index (PDI) was calculated to evaluate size distribution. HPLC assay was performed for determination of drug loading content (DLC) of both drugs and entrapment efficiency (EE). The *in vitro* drug release from nanomicelles was evaluated by a dialysis method as reported previously.[29] Briefly, the total DOX concentration was set at 0.2 mg/mL, and the PBS solution containing 1% polysorbate 80 (pH 7.4) was used as release medium for incubation at 37°C. At pre-set intervals, the sample outside dialysis bag with a molecular weight cut-off of 8–10 kDa (Shanghai Yuanye Biotechnology Co., Ltd., China) was withdrawn and mixed with mobile phase for HPLC analysis to determine the amount of drug release for calculation of *in vitro* drug release rate.

Formula optimization

Design of experiment (DOE) was performed for formula optimization of CPMSD via Box-Behnken design (BBD) method due to the high efficiency with small numbers of tests.[30] Design-Expert® (Version 8.0.6, State-Ease Inc., Minneapolis, MN, USA) was applied for a three-factor-three-level BBD, which included the major independent variables such as polymer type (X_1), mass ratio of DOX to SAA (X_2), and drug feed ratio (X_3) as displayed in Table 1. The dependent variables were particle size (Y_1), drug loading (Y_2) and entrapment efficiency (Y_3), and the design matrix containing a total of 17 experimental runs were obtained as shown in Table 2.

Molecular dynamics simulation

Molecular dynamics simulation was performed to investigate the molecular mechanism of drug entrapment into micelles by using the open source HyperChem software (Professional 80, Hypercube Inc., Gainesville, USA). At first, the 3-D structure of copolymer or small-molecule drug was theoretically simulated by means of molecular mechanics (MM) and molecular dynamics (MD).[21] According to the initial structure, a series of geometrical optimization then were performed at MM level via OPLS method by using the steepest descent algorithm until the root mean square gradient was less than 0.10 kcal / (mol•Angstrom). After heating from 0 K to 600 K, the optimized structure then was subject to a series of MD simulations running at 600 K with each runtime of 100 ps to obtain a lower energy minimum, for which the CHARMM27 force field was used and the solvent effect was considered implicitly.[31, 32] Finally random docking was performed to examine the interactions among drug and copolymer based on the optimal 3-D structures of copolymer and small-molecule drug (DOX or SAA).

Assessment of in vitro cytotoxicity and cell uptake

The *in vitro* cytotoxicity against MCF-7 cells was evaluated by using the Cell Counting Kit-8 (CCK-8, Dalian Meilun Biotech Co., Ltd, China). Briefly, the cells in logarithmic growth phase were prepared as single cell suspensions, and seeded into 96-well plates at a density of 4×10^3 per well for pre-incubation overnight. Then the cells were subjected to different treatment paradigms for 24 h incubation. Drug was aspirated and PBS (pH 7.4) was used to rinse cells thrice, then cell viability assessment was performed according to the kit manual by recording the absorbance of medium with CCK-8 (10%, v/v) after 6 h incubation via a

microplate reader at 450 nm. All the results were the average measurement of six replicate wells and were expressed as mean ± SD.

For cell uptake studies, the MCF-7 cell line was inoculated on a glass petri dish (35 mm×12 mm, 1×10^5 cells/mL) for 24 h. After removal of the spent medium, fresh DMEM medium containing drug at an equivalent DOX concentration of 0.2 μM was placed and cells were incubated for 2 h. Then the medium was aspirated, the cells were rinsed thrice with PBS (pH 7.4) and then put in 4% paraformaldehyde fix solution for 15min. After discarded the fix liquid, cells were rinsed thrice with PBS. After operated procedures above, the cells were further incubated in DAPI solution for 15 min. After removal of the dye, cells were rinsed thrice with PBS and subjected to observation under a confocal laser scanning microscopy (CLSM).

In vivo studies using a murine xenograft model

The xenograft tumor model in nude mice was established by subcutaneously inoculating human breast cancer MCF-7 cells (4×10^7 cells),[33] the tumor-bearing mice with the volume of solid tumors reached 170 ~ 200 mm^3 then were randomized into four groups ($n = 8$), and i.v. administered once every 2 days for repeated 5 times with various formulations, namely, CPMSD micelles, free DOX solution, the cocktail solution of free DOX and SAA, or the vehicle as a negative control. For each administration, normal saline was used as a vehicle and the dosage was 2.5 mg/kg for DOX and 10 mg/kg for SAA equivalent.[21] At 24 h after the last dosing, blood samples were collected to prepare serum for further biochemical estimations, then all the mice were sacrificed and tumors and major tissues were immediately harvested, weighted and stored for further analysis.

Quantitation, data analysis and statistics

Drug content in micelles was determined by HPLC-UV method using a Waters e2695 HPLC system. The chromatographic separation was performed on a TC-C18 column (250 mm ×4.6 mm, 5μm) at 30°C via isocratic elution with the mixture of methanol and 0.2% aqueous formic acid (55/45, *v/v*) at a flow rate of 1.0 mL/min, and the detection wavelength was 420 nm for DOX, and 254 nm for SAA, respectively. UPLC-MS/MS assay was performed to determine drug content in biosamples such as plasma and tissues by using an AB Sciex Triple Quad™ 4500 system connected with Shimadzu LC-30AD via electro-spray ionization (ESI) interface. The mass spectrometer was operated in positive mode by using multiple reaction monitoring (MRM) of the transitions *m/z* 544.2/396.8 for DOX and *m/z* 749.4/591.5 for the internal standard azithromycin, while in negative mode using the transitions *m/z* 493.2/294.9 for SAA and *m/z* 367.0/149.0 for the internal standard curcumin, respectively.

Colorimetric assays were performed by using commercial kits to evaluate major markers of cardiotoxicity such as lactate dehydrogenase (LDH), creatine kinase (CK) and cardiac troponin T (cTnT) in serum, and malondialdehyde (MDA), superoxide dismutase (SOD) in cardiac tissue. For histological examination, the paraffin-embedded sections of the left half heart of mice were sliced (5 μm) and then HE staining for light

microscope observations was performed. All specimens were analyzed, and the representative images were captured by two pathologists with blind investigation.

All data were presented as mean ± standard deviation (SD) of replicate measurements. Student's *t*-test was applied to statistical analysis of experimental data by using the statistical software package SPSS 20.0 (International Business Machines Corporation, New York, USA). Statistical significance was indicated by $p < 0.05$ and more statistical significance by $p < 0.01$.

Results And Discussion

Optimal formulation of CPMSD based on DOE

Taking into consideration the fact that Box-Behnken design (BBD) method has been widely applied in DOE due to the high efficiency with small numbers of tests,[30] a 3-factor-3-level BBD was performed herein for optimizing the formulation of CPMSD. As shown in Table 1, the independent variables were some crucial factors concerned with complex polymeric micelles fabrication such as the types of polymer (X_1), mass ratio of DOX to SAA (X_2) and the feed ratio of carrier to drugs (X_3), for which the corresponding levels were set according to preliminary one-factor tests for screening. More to the point, three common used amphiphilic block copolymers were applied for micellar formula optimization, namely mPEG-PLA, mPEG-PCL, and mPEG-PCL-Phe (Boc), wherein the hydrophilic segment was mPEG with an average molecular weight of about 2,000, and the hydrophobic segment was selected from polylactide (PLA), polycaprolactone (PCL), or that capped with N-*t*-butoxycarbonyl-phenylalanine (Boc-Phe). All these copolymers were synthesized and characterized in our lab, and the drug entrapment properties had been well demonstrated in previous studies.[21, 29, 30] Resultantly, the design matrix containing a total of 17 experimental runs were obtained from BBD as shown in Table 2, which contained 12 factorial points at the midpoint of edge for each process space, and 5 replicates at the center point for estimation of pure error sum of squares. Each experimental run then could be performed in light of the design matrix in random order to avoid bias.

Table 1 Independent variables and levels involved in Box-Behnken design

Independent variable	Level		
	Low (-1)	Medium (0)	High (+1)
X_1 Types of polymer	mPEG-PLA	mPEG-PCL	mPEG-PCL-Phe(Boc)
X_2 Mass ratio of DOX/SAA	1:2	1:4	1:6
X_3 Feed ratio	4:1	5:1	8:1

Table 2 Box-Behnken experimental design and the observed responses

Run	Independent variable			Dependent variable		
	X_1	X_2	X_3	Y_1 (nm)	Y_2 (%)	Y_3 (%)
1	0	0	0	17.11 ± 1.30	13.3 ± 0.4	85.6 ± 4.8
2	0	-1	-1	18.78 ± 0.75	14.5 ±1.0	75.0 ± 2.1
3	0	+1	+1	17.65 ± 0.97	4.5 ± 0.6	43.0 ± 2.0
4	0	0	0	16.99 ± 1.12	13.4 ± 1.1	92.9 ± 3.3
5	0	0	0	16.98 ± 0.90	13.9 ± 1.5	100.4 ± 4.2
6	0	-1	+1	17.66 ± 2.11	8.0 ± 0.7	80.6 ± 5.2
7	0	0	0	16.82 ± 2.01	15.1 ± 1.0	101.6 ± 15.0
8	+1	+1	0	17.16 ± 1.01	16.5± 1.2	101.8 ± 2.8
9	-1	-1	0	224.5 ± 22.34	11.7 ± 0.7	87.8 ± 4.6
10	-1	0	+1	15.03 ± 1.67	9.9 ± 0.6	78.9 ± 6.7
11	0	+1	-1	16.77 ± 0.52	19.8 ± 1.5	96.1 ± 8.7
12	+1	0	-1	18.44 ± 0.73	16.6 ± 1.7	87.7 ± 5.3
13	+1	-1	0	266.9 ± 24.21	11.7 ± 0.7	72.7 ± 6.5
14	+1	0	+1	18.23 ± 1.31	10.6 ± 0.5	93.9 ± 8.0
15	0	0	0	17.46 ± 0.63	15.7 ± 1.2	91.6 ± 11.3
16	-1	+1	0	16.06 ± 0.37	15.0 ± 1.4	84.9 ± 7.8
17	-1	0	-1	115.5 ± 9.78	14.6 ± 0.9	61.7 ± 9.1

It is well known that the dimensional characteristics of nanomicelles may contribute to passive targeting to tumor through the enhanced permeability and retention (EPR) effect, since it preferred to avoid macrophages uptake and clearance by mononuclear phagocyte system (MPS) or the reticuloendothelial system (RES), and achieved long circulation and fairly high chance of reaching tumor site. Furthermore, the nanomicelles with high DLC and EE but small particle size are usually expected to avoid immune clearance and maintain desired systematic bioavailability.[34] Herein, several key performance indices (KPI) of micellar system thus were used as the dependent variables for statistical analysis and evaluation of CPMSD formulation, namely particle size (Y_1), drug loading capacity (DLC, Y_2), and entrapment efficiency (EE, Y_3). The observed responses of KPI (Table 2) clearly revealed that there was significant differentiation among these experimental runs. Specifically, the particle size ranged from 15 nm to 267 nm, while DLC and EE changed between 4.5% and 19.8%, and 43.0% and 101.8%, respectively. The influence of all these independent variables (X_1, X_2, X_3) on KPI were further investigated by using multiple regression analysis. The cubic polynomial regression model for each KPI could be obtained with

determination coefficient (R^2) more than 0.9 and the *p*-value less than 0.05, and the 3-D response surface plots illustrated overall influence of the independent variables (Fig. 2 A-C). Among all the three formulation factors involved in the present study, X_3, namely the feed ratio of copolymer carrier to both drugs, was found to be the most important one for fabricating CPMSD micelles, especially had a great impact on DLC and EE. According to these results, all the three factors X_1, X_2 and X_3 thus were determined at the medium level for fabricating CPMSD micelles. That is to say, the multifunctional nanomicellles of CPMSD could be achieved by using the amphiphilic block copolymer of mPEG-PCL as a carrier for encapsulating both drugs under a carrier-drug mass ratio of 5:1 and DOX-SAA mass ratio of 1:4.

On the basis of optimal formulation obtained from BBD study, several batches of CPMSD nanomicelles were prepared by conventional thin film hydration technique, then characterized for verification.[21] DLS assay clearly demonstrated that the CPMSD micelles were usually the uniform and small particles with mean particle size ranging within 15 to 25 nm and the PDI values less than 0.2. Meanwhile, HPLC quantitation indicated that the DLC values for DOX and SAA together were (15.7 ± 0.8) %, and EE values were generally more than 95%. All these KPI values determined were in close agreement with the predicted values of optimal micellar system of CPMSD from DOE model that showed particle size of 17.1 nm, DLC of 14.3%, and EE of 94.4%, suggesting that the DOE-based optimal formulation would be reliable for fabricating the aimed dual drug-loaded nanomicelles of CPMSD for further evaluation.

Molecular mechanism of drugs entrapment into micelles

The possible mechanism of amphiphilic block copolymer encapsulating both drugs to form novel nanomicelles of CPMSD was further investigated in the present study. The approaches of molecular mechanics (MM) and molecular dynamics (MD) were applied to examine molecular interactions among the polymeric carrier (mPEG-PCL) and small-molecule drugs (DOX and SAA) based on simulating their theoretical structures.[31, 32] As illustrated in Fig. 3 (a-d), the copolymer initially displayed a curvilinear conformation, then gradually bended and changed with the heating process, finally formed into a spherical shape after 100ps MD simulation, which consisted of hydrophilic and hydrophobic parts and provided suitable binding sites for small molecules. Meanwhile, both small-molecule drugs constantly adjusted the conformation and distance from copolymer to obtain favorable interaction modes (Fig. 3 e-h). Resultantly the copolymer encapsulated SAA into the hydrophobic cavity and DOX to the hydrophilic surface, respectively (Fig. 3 i).

Chemically DOX is a kind of antibiotics with the amino sugar linked to anthracycline via a glycosidic bond (Fig. 1), which contributes to its hydrophilicity and the preference for binding to the hydrophilic surface of the copolymer mPEG-PCL. In contrast, SAA is a kind of salvianolic acid with fairly high hydrophobicity, thus could tight bind with the hydrophobic cavity of the copolymer. More to the point, the phenolic hydroxyl and carboxyl groups in SAA (Fig. 1) would significantly enhance the molecular interaction with the other drug molecule DOX via its basic amino sugar. From this point of view, SAA plays an important role as a bridge between DOX and the copolymer, which greatly promotes copolymer-

drug interaction, and leads to significant increase in drug encapsulation efficiency of the complex micellar system CPMSD, especially for the relatively hydrophilic drug molecule DOX. The findings from MD simulation clearly demonstrated that CPMSD could act as a new and efficient dual drug-loaded micellar DDS by a unique mechanism involved in drug entrapment, which might also result in specific drug release profiles of CPMSD.

Colloidal properties and stability of CPMSD

Polymeric nanomicelles are a kind of self-assembled colloidal particles for drug delivery, and the colloidal stability has a great impact on pharmaceutical performance such as *in vitro* and *in vivo* drug release behaviors.[35] Therefore the colloidal properties and stability of CPMSD were investigated through observation of appearance and particle size. As illustrated in Fig. 4A, the nanomicelles of CPMSD fabricated under the optimal formulation presented as a stable colloidal suspension clearly displaying a Tyndall effect, and lyophilization could provide a yellowish red powder with good disparity without collapse or atrophy, as well as good re-dispersibility in saline, PBS or double distilled water. The TEM image for morphology further revealed that CPMSD micelles were uniform nanoparticles with spherical or nearly spherical shape and a typical particle size of about 20 nm (Fig. 4B).

In order to know the colloidal stability of CPMSD micelles, how the particle size changed with temperature was investigated at first. Six batches of fresh prepared micelles (2 ml/branch) were divided into two groups (n=3) and placed at 4 °C and room temperature (25°C), respectively, then the particle size was monitored periodically. Although a significant increase in particle size was observed after storage at 4 °C for 12 hrs, the fresh prepared CPMSD could maintain a stable micellar particle size for at least 24 hrs at room temperature (Fig. 4C), suggesting a reliable condition to produce lyophillized powder of CPMSD for storage.

The particle size change in simulated serum was further inspected to evaluate the colloidal stability of CPMSD in systemic circulation. The micelles were incubated with fetal bovine serum (FBS, pH 7.4) at 37 °C under gentle stirring, and an aliquot of the sample was withdrawn for the measurement according to the time schedule. As shown in Fig. 4D, there was no significant change with time in micellar particle size within 24 hrs incubation in the simulated body fluid containing 1% or 10% FBS ($p > 0.05$), indicating a good colloidal stability of CPMSD *in vivo*. Meanwhile, the CPMSD micellar particles in PBS displayed a slightly negative zeta potential, i.e. – (1.77±0.49) mV, and this value became more negative with increasing FBS content, namely – (3.20±0.53) mV and – (3.62±0.27) mV in the incubation system containing 1% FBS, and 10% FBS, respectively. These findings together demonstrated the coating effect of endogenous proteins such as serum albumin might be chiefly responsible for *in vivo* colloidal stability of CPMSD.

In vitro drug release from CPMSD

The *in vitro* drug release characteristics of CPMSD were investigated via dialysis method, and PBS solution containing 1% Tween 80 (pH 7.4) was used as the release medium to maintain the chemical

stability and sink condition for both DOX and SAA. Resultantly, there was significant difference in the *in vitro* release profile between DOX and SAA (Fig. 5). Although the encapsulated drugs were both sustained released from CPMSD, DOX had a much higher release rate at early stage than SAA did, and an initial release burst with a percent cumulative release of 45% within 0.5 h could be observed. The drug release of DOX increased steadily, and the cumulative drug release amount reached a peak of about 90% within 3 hrs. In contrast, the nanomicelles of CPMSD constantly released SAA at a rather slow rate, which had a percent cumulative release up to 70% within 72 hrs.

Furthermore, the kinetic mechanism of drug release from CPMSD was investigated by fitting several common kinetic models to the cumulative release profiles, including the zero-order, first-order and Higuchi models. As shown in Table 3, the first-order model was determined as the optimal one with the highest goodness of fit, and the values of determination coefficient (R^2) reached up to 0.97 for both drugs. Thus, it could be concluded that non-constant diffusion was the chief mechanism involved in drug release from CPMSD micelles for both DOX and SAA, while matrix swelling and dissolution could be negligible in the present dual drug-loaded polymeric micellar system. All these findings clearly demonstrated the special drug releasing characteristics of CPMSD, and also provided a strong evidence for the above-mentioned distinctive mechanism of drug entrapment based on MD studies, which thought that CPMSD micelles would be prone to a relatively fast drug release for DOX from the hydrophilic surface, but an extended release for SAA from the inner core.

Table 3 Model fitting for in vitro drug release from nanomicelles of CPMSD micelles

Model	DOX*	SAA*
Zero-order equation	Y=0.78t+71.07 (0.2103)	Y=0.86t+21.50 (0.7811)
First-order equation	Y=87.66[1-exp(-1.26t)] (0.9819)	Y=65.18[1-exp(-0.10t)] (0.9765)
Higuchi equation	$Y=6.36t^{1/2}+61.67$ (0.4924)	$Y=8.55t^{1/2}+7.05$ (0.9402)

Notes: * The data in parenthesis were the determination coefficient for model fitting.

In vitro cytotoxicity and cellular uptake

The *in vitro* cytotoxicity activity of CPMSD against human breast cancer MCF-7 cells was evaluated by using CCK-8 assay of cell viability. Several relative preparations were used for comparison, including free solution of DOX, SAA and the cocktail formulation of DOX and SAA. Free DOX alone could significantly inhibit *in vitro* proliferation of MCF-7 cells in a concentration-dependent manner with the final concentration ranging within 0.01 ~ 5 μM (Fig. 6A), and the half inhibitory concentration (IC_{50}) was determined as 0.27 μM, which was in good consistence with the data previously reported and demonstrated the high potency of DOX as a chemotherapy agent for human breast cancer.[36]

Fig. 6B clearly illustrated the difference in cytotoxicity against MCF-7 cells among various treatments involved. More to the point, free DOX alone at a final concentration of 230 ng/ml close to the IC_{50} value

caused an inhibition rate of ~ 60% against *in vitro* growth of MCF-7 cells. The treatment with CPMSD preparation or DOX-SAA cocktail displayed a similar inhibition rate to free DOX at the same concentration, and no significance difference was observed among the three groups ($p > 0.05$). In contrast, the treatment with free SAA alone only yielded ~ 40% inhibition at a final concentration of 930 ng/ml, which was set four times as much as DOX according to their mass ratio in CPMSD (1:4). Furthermore, the inhibition rate of SAA treatment was found to be quite lower than that of free DOX alone or DOX-SAA combination via the CPMSD preparation ($p < 0.05$). These findings demonstrated that neither copolymer entrapment nor the combination with SAA would have significant effect on the inhibitory potency of DOX against MCF-7 cells growth, and DOX thus could be regarded as the major active pharmaceutical ingredient responsible for anticancer efficacy of the present CPMSD nano-formulation used for cancer chemotherapy.

DOX is an anthracycline drug widely used in breast cancer chemotherapy. So far, the best-known and widely accepted mechanisms are based on the inhibition of DNA replication, transcription and repair processes, which is mediated by the drug intercalation into DNA and occur in the nucleus.[37] The final target location of DOX is the nucleus, which is usually regarded as the main target responsible for the anticancer potency of DOX.[38] The cellular uptake of DOX and the effect of CPMSD formulation thus were investigated following the evaluation of anticancer potency *in vitro*. Cell nuclei were *stained by DAPI, and* CLSM was employed for observation through detecting its blue fluorescence and the obvious specific red fluorescence of DOX. Continuous increase in the fluorescence intensity of DOX could be clearly observed with extension of the incubation time. After a 2-h incubation, all the three groups treated with DOX at an equivalent concentration displayed similarly strong red fluorescence when compared with the control group without any drug treatment. According to the Merge column, the regions with red fluorescence of DOX were well overlapped with those with blue fluorescence of DAPI and there was no significant difference among these DOX containing treatments (Fig. 6C), indicating a rapid uptake of DOX almost entirely into the nuclei of MCF-7 cells, no matter what the preparation of DOX was. The results from *in vitro* evaluation together revealed that the CPMSD preparation might be an efficient nano-formulation of DOX with full maintenance of the anticancer potency and the final target of this chemotherapy drug.

In vivo anticancer efficacy

Female BALB/c nude mice bearing human breast cancer MCF-7 cells were employed to evaluate *in vivo* therapeutic responses of the CPMSD preparation such as anticancer efficacy, as well as the protective effect against DOX-induced cardiotoxicity. All the model mice were randomly divided into several groups (n=8) administering different formulations of DOX under the same regime, and the anti-tumor therapeutic efficacy was assessed through characterizing the tumor with time after administration. More specifically, the aim drug DOX, which was delivered by the free drug alone, CPMSD or the cocktail formulation both with a DOX/SAA mass ratio of 1:4, was intravenously administered at a single DOX dose of 2.5 mg/kg for five times every each other day.[21] The mice only given the same volume of vehicle (saline) was used as the negative control (NC) for comparison.

In contrast to the mice in NC group, the animals administered DOX all had drastic inhibition of tumor growth, no matter what the drug formulation was. As illustrated in Fig. 7A, tumor grew gradually in the NC group and the relative tumor volume reached 150% after the last injection of saline, whereas the other three groups (DOX, Cocktail and CPMSD) similarly showed an opposite temporal profile and all displayed a significant difference from the NC group in the relative tumor volume ($p < 0.01$). After the accomplishment of all the five DOX dosages, the relative tumor volume was observed ranging from less than 40% to about 50%, which varied with the formulations of DOX. Moreover, significant difference among these DOX formulations could be found after the second dosage, and some tumors were even completely eradicated through treatment by the CPMSD micelles. Since it would take time for the micelles to penetrate into tumors, concentrate at the tumor site and release drug,[36] these findings thus indicated that CPMSD might be a kind of sustained release preparation of DOX with tumor-targeting efficiency, as well as the most potent DOX formulation against breast cancer growth in mice.

In order to confirm the observation of tumor volume changes, all the mice were sacrificed one day after the last dosage and tumors were resected and weighed. As shown in Fig. 7B, the tumor weight averaged 70.1±11.5 mg for the mice in NC group, 25.9±5.6 mg for DOX group, 30.5±7.2 mg for Cocktail group, and 27.4±8.7 mg for CPMSD group, respectively. The mice only treated by saline showed the maximum mean tumor weight, while all the DOX-containing treatments, no matter what the drug formulation was, led to dramatic shrinkage of the tumor weight in comparison with that in the NC group ($p < 0.01$). Then the tumor growth inhibition (TGI) was calculated to quantify treatment effects. The TGI value for antitumor activity rating reached up to 63.0% by free DOX alone, 56.5% by the cocktail formulation of DOX, and 60.9% by CPMSD preparation, respectively, and there was no significant difference among these DOX formulations ($p > 0.05$).

Meanwhile, the body weight was monitored for each animal to investigate the potential difference in systemic toxicity among various treatments. Although the mice in each group had a similar mean body weight till the second dosage, significant difference could be observed among the three DOX formulations involved after finishing all the five dosages ($p < 0.01$), and the final body weight of the mice in CPMSD group was the closest to that in NC group (Fig. 7C), suggesting excellent biosafety of this DOX formulation. Therefore, it was concluded that co-treatment with SAA by CPMSD micelles or the simple cocktail would not attenuate *in vivo* antitumor potency of DOX, and its systemic toxicity could be greatly alleviated by the CPMSD formulation. Indeed, distinctive differences could be observed in bio-distribution characteristics (Fig. 8) between the dual drug-loaded polymeric micellar system of CPMSD and the simple cocktail formulation of free DOX and SAA, which revealed the site-specific drug releasing properties of CPMSD and therefore the possible mechanisms responsible for its high antitumor potency and low toxicity *in vivo*.

In vivo protective effects against cardiotoxicity

The clinical use of DOX is limited by severe cardiotoxic side effects, although it is a potent anticancer drug. Oxidative stress is generally recognized as one of the main mechanisms responsible for DOX

induced cardiotoxicity and much research has recently been devoted to this challenge, mainly including some doxorubicin-antioxidant co-drugs,[39] and dual drug-loaded nano-platform for targeted cancer therapy toward clinical therapeutic efficacy of multifunctionality.[40] Our present study aimed at the CPMSD formulation *for breast cancer chemotherapy*, which was a high-performance multifunctional polymeric micellar delivery system co-loading the anticancer drug DOX and the highly potent natural antioxidant SAA. Following evaluation of antitumor efficacy, the detoxication effect of SAA delivered by CPMSD was further investigated in tumor-bearing nude mice through assay of several principal physiological and biochemical markers related to myocardial function, as well as inspection of myocardial histologic changes concerned with cardiotoxicity.

Along with monitoring body weight changes, the heart weight of each animal was measured for calculating the cardiac weight index (CWI) by its ratio to body weight. As shown in Fig. 9A, the NC group had a maximum CWI value of (0.48±0.01) %, while the minimum value was found as (0.34±0.03) % for the mice administered free DOX alone. Significant difference in CWI could be observed between the NC group and any of the other two groups treated with DOX-containing formulation but CPMSD at an equivalent dosage ($p < 0.01$). There was no significant difference between the DOX and cocktail group, even though it was co-administered with the antioxidant agent SAA through the cocktail formulation. However, the CWI value for the mice administered CPMSD micelles was found as (0.46±0.02) %, which was significantly higher than the other two DOX-containing groups ($p < 0.01$), and even close to that in the NC group ($p > 0.05$). Taking into consideration of the changes in both CWI and body weight (Fig. 7C), these results thus indicated the differentiated effect of co-treatment formulation on DOX induced cardiotoxicity and the effectiveness of CPMDC that could nearly bring the two major physiological indexes back to normal.

In order to quantitatively evaluate the protective efficacy of CPMSD against *cardiotoxic* side effects caused by DOX dosing, biochemical analysis was further performed on the crucial markers involved in cardiac toxicity, including SOD and MDA in heart tissues, and LDH, CK and cTnT in plasma.[5, 21] When compared with the NC group, the mice administered free DOX alone showed significantly decreased SOD level along with elevated MDA content ($p < 0.01$), suggesting the DOX-induced oxidative injury and remarkable amelioration of co-administration of SAA through the CPMDC formulation (Fig. 9B). Meanwhile, significant increases in plasma level of LDH, CK and cTnT could correspondingly be observed in the mice administered free DOX alone or the simple cocktail of DOX and SAA (Fig. 9C), which confirmed the occurrence of cardiac injury in both DOX and cocktail group. Comparison among these DOX-containing formulations further revealed the reducing effect on all these markers of co-treatment with SAA by CPMDC, but not the cocktail of free DOX and SAA ($p < 0.01$). Due to the effective protection against DOX induced cardiotoxicity, it therefore was concluded that the tumor-bearing mice would greatly benefit from the present CPMSD formulation of DOX and SAA into dual drug-loaded polymeric micelles.

Finally, the histopathological examination of cardiac tissue specimens was performed to manifest DOX-induced toxic injuries on the main target organ. As illustrated in Fig. 9D, the tumor-bearing nude mice in NC group showed basically normal morphology of cardiac myocyte in the left ventricle, while the DOX-

containing treatments could affect cardiomyocytes in different ways and to different degrees depending on the formulation, among which the severest myocardial damage was observed in the mice only treated with free DOX. Accompanied by infiltration of inflammatory cells, the DOX alone group exhibited obvious myocardial injuries such as cross-striations, myocardial endochylema puffing and sarcoplasmic matrix partly resorbed, as well as myocardial fiber disarrangement, cellular swelling and degeneration, hinting toward toxin-mediated necrosis of cardiomyocytes. More to the point, these DOX-induced cardiomyocytes injuries could be alleviated by co-administering SAA, especially through the CPMSD micelles, which displayed less histopathological changes than the cocktail formulation at an equivalent dosage. These findings altogether demonstrated the high potency of SAA against cardiotoxic effect of DOX by co-administering both drugs through the CPMSD formulation.

Conclusions

The present study was an important part of finding efficient strategies for high-performance chemotherapy of breast cancer. By using biocompatible copolymer carrier, CPMSD was developed as an advanced multifunctional polymeric micellar delivery system co-loading the anticancer drug DOX and potent natural antioxidant SAA to overcome the dose-dependent cardiotoxicity associated with cancer therapy. Based on optimal formulation, the complex polymeric micelles CPMSD could be constructed by colloidal self-assembly of the amphiphilic copolymer of mPEG-PCL, which integrated SAA into the hydrophobic cavity and bound DOX to the ball-shaped surface. CPMSD was demonstrated to have favorable physico-pharmaceutical properties, as well as the specific effect of killing two birds with one stone by maintaining the anticancer efficacy of DOX against the associated cardiotoxicity, which thus provide it a great promise for clinical translation as an improved nano-formulation of the well-known anticancer drug. Further investigations would be focused on drug-drug interactions that play a pivotal role in combination therapy.

Abbreviations

DOX: Doxorubicin; SAA: Salvianolic acid A; IARC: International Agency for Research on Cancer; WHO: World Health Organization; TNBC: Triple-negative breast cancer; FDA: Food and Drug Administration; ROS: Reactive oxygen species; PMs: polymeric micelles; CPMSD: Compound micelles of DOX and SAA; PBS: Phosphate-buffered solution; PDI: Polydispersity index; DLC: Drug loading content; EE: Entrapment efficiency; DOE: Design of experiment; BBD: Behnken design; MM: Molecular mechanics; MD: Molecular dynamics; CLSM: Confocal laser scanning microscopy; ESI: Electro-spray ionization; MRM: Multiple reaction monitoring; LDH: Lactate dehydrogenase; CK: Creatine kinase; cTnT: Cardiac troponin T; MDA: Malondialdehyde; SOD: Superoxide dismutase; PLA: Polylactide; PCL: Polycaprolactone; EPR: Enhanced permeability and retention; MPS: Mononuclear phagocyte system; RES: Reticuloendothelial system; KPI: Key performance indices; IC50: Half inhibitory concentration; NC: Negative control; TGI: Tumor growth inhibition.

Declarations

Acknowledgments

Not applicable.

Authors’ contributions

Conceptualization, ZL, HX and HW; Data curation, ZL, JL and ZS; Formal analysis, ZL and JL; Funding acquisition, HX and HW; Investigation HX; Methodology, ZL, ZS and YL; Project administration, HX, HW and FZ; Software, ZS and BY; Supervision, HX, ZL and HW; Validation, HX and YL; Visualization, HX, ZL and ZS; Writing—original draft, ZL and JL; Writing—review & editing, HX and FZ. All authors have read and agreed to the published version of the manuscript.

Funding

This work was supported by the National Natural Science Foundation of China (82073888), Science and Technology Support Program for Youth Innovation in Universities of Shandong (2019KJM009), Natural Science Foundation of Shandong Province (No. ZR2019MB054), Science and Technology Project of TCM in Shandong Province (No. 2020Z37, 2020M190), Graduate Innovation Foundation of Yantai University (GIFYTU No. YDZD2031), and the Top Talents Program for One Case Discussion of Shandong Province, China.

Availability of data and materials

The datasets used and analyzed during the current study are available from the corresponding author on reasonable request.

Ethics approval and consent to participate

All animal experimental procedures were conducted by following the National Institutes of Health (NIH) guidelines and approved by the Animal Experimentation Ethics Committee of Yantai University, China.

Consent for publication

All authors agree to publish this manuscript in this journal.

Competing interests

The author reports no conflicts of interest in this work.

References

1. Bray F, Ferlay J, Soerjomataram I, Siegel RL, Torre LA, Jemal A (2018) Global cancer statistics 2018: GLOBOCAN estimates of incidence and mortality worldwide for 36 cancers in 185 countries. CA Cancer J Clin 68:394–424.
2. Waks AG, Winer EP (2019) Breast cancer treatment: A review. JAMA 321: 288–300.
3. Blum JL, Flynn PJ, Yothers G et al (2017) Anthracyclines in early breast cancer: the ABC Trials-USOR 06–090, NSABP B-46-I/USOR 07132, and NSABP B-49 (NRG Oncology). J Clin Oncol 35 (23): 2647–2655.
4. Chatterjee K, Zhang J, Honbo N, Karliner JS (2010) Doxorubicin cardiomyopathy. Cardiology 115(2): 155–162.
5. Ewer MS, Ewer SM (2010) Cardiotoxicity of anticancer treatments: what the cardiologist needs to know. Nat Rev Cardiol 7 (10): 564–575.
6. Duggan ST, Keating GM (2011) Pegylated liposomal doxorubicin. A review of its use in metastatic breast cancer, ovarian cancer, multiple myeloma and AIDS-related Kaposi's sarcoma. Drugs 71 (18): 2531–2558.
7. Cvetković RS, Scott LJ (2005) Dexrazoxane: a review of its use for cardioprotection during anthracycline chemotherapy. Drugs 65 (7): 1005–1024.
8. Kane RC, Mcguinn WD, Dagher R, Justice R, Pazdur R (2008) Dexrazoxane (Totect™): FDA review and approval for the treatment of accidental extravasation following intravenous anthracycline chemotherapy. Oncologist 13 (4): 445–450.
9. Shaikh F, Dupuis LL, Alexander S, Gupta A, Mertens L, Nathan PC (2016) Cardioprotection and second malignant neoplasms associated with dexrazoxane in children receiving anthracycline chemotherapy: A systematic review and meta-analysis. J Natl Cancer Inst 4: 46–69.
10. Spalatoceruso M, Napolitano A, Silletta M et al (2019) Use of cardioprotective dexrazoxane is associated with increased myelotoxicity in anthracycline-treated soft-tissue sarcoma patients. Chemotherapy 64(2):1–5.
11. Mitry MA, Edwards JG (2016) Doxorubicin induced heart failure: Phenotype and molecular mechanisms. Int J Cardiol Heart Vasc 10: 17–24.
12. Kaiserova H, Simunek T, van der Vijgh WJ, Bast Aalt, Kvasnickova E (2007) Flavonoids as protectors against doxorubicin cardiotoxicity role of iron chelation, antioxidant activity and inhibition of carbonyl reductase. Biochimica et Biophysica Acta 1772 (9): 1065–1074.
13. Sun GB, Wang J, Zhang MD, Sun XB (2017) Salvianolic acid B attenuates doxorubicin-induced ER stress by inhibiting TRPC3 and TRPC6 mediated Ca2 + overload in rat cardiomyocytes. Tocical Lett

276: 21–30.

14. Benzer F, Kandemir FM, Ozkaraca M, Kucukler S, Caglayan C. Curcumin ameliorates doxorubicin-induced cardiotoxicity by abrogation of inflammation, apoptosis, oxidative DNA damage, and protein oxidation in rats. J Biochem Mol Toxicol. 2018; e22030.
15. Guo Z, Yan M, Chen L et al (2018) Nrf2-dependent antioxidant response mediated the protective effect of tanshinone IIA on doxorubicin-induced cardiotoxicity. Exp Ther Med 16: 3333–3344.
16. Torchilin VP (2007) Micellar nanocarriers: pharmaceutical perspectives. Pharm Res 24 (1): 1–16.
17. Gong C, Deng S, Wu Q et al (2013) Improving antiangiogenesis and anti-tumor activity of curcumin by biodegradable polymeric micelles. Biomaterials 34 (4):1413–1432.
18. Wicki A, Witzigmann D, Balasubramanian V, Huwyler J (2015) Nanomedicine in cancer therapy: challenges, opportunities, and clinical applications. J Control Release 200:138–157.
19. Cagel M, Tesan FC, Bernabeu E et al (2017) Polymeric mixed micelles as nanomedicines: Achievements and perspectives. Eur J Pharm Biopharm 113: 211–228.
20. Ramasamy T, Ruttala HB, Chitrapriya N et al (2017) Engineering of cell microenvironment-responsive polypeptide nanovehicle co-encapsulating a synergistic combination of small molecules for effective chemotherapy in solid tumors. Acta Biomater 48:131–143.
21. Zhang D, Xu Q, Wang N et al A complex micellar system co-delivering curcumin with doxorubicin against cardiotoxicity and tumor growth. Int J Nanomed 13: 4549–4561.
22. Lin TJ, Liu GT, Liu Y, Xu GZ (1992) Protection by salvianolic acid A against adriamycin toxicity on rat heart mitochondria. Free Radical Bio Med 12 (5): 347–351.
23. Fan HY, Yang MY, Qi D et al (2015) Salvianolic acid A as a multifunctional agent ameliorates doxorubicin-induced nephropathy in rats. Sci Rep 5:12273.
24. Fan HY, Yang L, Fu FH et al (2012) Cardioprotective effects of salvianolic acid A on myocardial ischemia-reperfusion injury in vivo and in vitro. Evid-Based Compl Alt 2012: 508938.
25. Hou B, Qiang G, Zhao Y et al (2017) Salvianolic acid A protects against diabetic nephropathy through ameliorating glomerular endothelial dysfunction via inhibiting AGE-RAGE signaling. Cell Physiol Biochem 44 (6): 2378–2394.
26. Zhou L, Zuo Z, Chow M S (2013) Danshen: an overview of its chemistry, pharmacology, pharmacokinetics, and clinical use. J Clin Pharmacol 53(12):787–811.
27. Shen Y, Wang XY, Xu LH, Liu XW, Chao RB (2009) Characterization of metabolites in rat plasma after intravenous administration of salvianolic acid A by liquid chromatography/time of-flight mass spectrometry and liquid chromatography/ion trap mass spectrometry. Rapid Commun Mass Sp 23 (12):1810–1816.
28. Xu H, Li YL, Che X, Tian HC, Fan HY, Liu K (2014) Metabolism of salvianolic acid A and antioxidant activities of its methylated metabolites. Drug Metab Dispos 42 (2): 274–281.
29. Liu H, Xu H, Jiang Y et al (2015) Preparation, characterization, in vivo pharmacokinetics, and biodistribution of polymeric micellar dimethoxycurcumin for tumor targeting. Int J Nanomedicine 10:

6395–6410.
30. Jiang YX, Wang F, Xu H, Liu H, Meng QG, Liu WH (2014) Development of andrographolide loaded PLGA microspheres: Optimization, characterization and in vitro–in vivo correlation. Int J Pharmaceut 475 (1–2): 475–484.
31. Jorgensen WL, Maxwell DS, Tirado-Rives J (1996) Development and testing of the OPLS all-atom force field on conformational energetics and properties of organic liquids. J Am Chem Soc 118 (45):11225–11236.
32. Foloppe N, MacKerell A (2000) All-atom empirical force field for nucleic acids: I. Parameter optimization based on small molecule and condensed phase macromolecular target data. J Comput Chem 21: 86–104.
33. Zuo JX, Jiang YM, Zhang EX et al (2019) Synergistic effects of 7-O-geranylquercetin and siRNAs on the treatment of human breast cancer. Life Sci 227: 145–152.
34. Li Z, Xiao C, Yong TY, Li ZF, Gan L, Yang XL (2020) Influence of nanomedicine mechanical properties on tumor targeting delivery. Chem Soc Rev 49 (8): 2273–2290.
35. Moore TL, Rodriguez-Lorenzo L, Hirsch V et al (2015) Nanoparticle colloidal stability in cell culture media and impact on cellular interactions. Chem Soc Rev 44 (17): 6287–6305.
36. Tsou SH, Chen TM, Hsiao HT, Chen YH (2015) A critical dose of doxorubicin is required to alter the gene expression profiles in MCF-7 cells acquiring multidrug resistance. PLoS ONE 10 (1): e0116747.
37. Szaflarski W, Sujka-Kordowska P, Januchowski R et al (2013) Nuclear localization of P-glycoprotein is responsible for protection of the nucleus from doxorubicin in the resistant LoVo cell line. Biomed Pharmacother 67 (6): 497–502.
38. Li X, Wu XH, Yang HY, Li L, Ye ZQ, Rao YF (2019) A nuclear targeted Dox-aptamer loaded liposome delivery platform for the circumvention of drug resistance in breast cancer. Biomed Pharmacother 117: 109072.
39. Chegaev K, Riganti C, Rolando B et al (2013) Doxorubicin-antioxidant co-drugs. Bioorg Med Chem Lett 23 (19): 5307–5310.
40. Ma Z, Li N, Zhang B et al (2020) Dual drug-loaded nano-platform for targeted cancer therapy: toward clinical therapeutic efficacy of multifunctionality. J Nanobiotechnol 18 (1): 123.

Figures

Figure 1

Schematic representation of the self-assembly of CPMSD and its multifunction for cancer therapy.

Figure 2

Response surface plots of DOE showing the effects of formulation on (A) particle size (B) drug loading capacity and (C) entrapment efficiency of CPMSD

Figure 3

Molecular dynamics simulation of drug entrapment into CPMSD. (a)-(d) MD simulation process of the copolymer (mPEG-PCL); (e)-(h) merging copolymer with drugs (DOX and SAA), DOX-yellow stick, SAA-purple- stick; (i) the final 3-D map of copolymer-drug interaction (copolymer- gray solid surface, DOX- blue stick, SAA- pink stick)

Figure 4

Characterization of CPMSD by (A) appearance observation (the lyophilized powder and micellar solution in saline), (B) TEM imaging (×150,000), (C) stability of particle size at 4℃ (●) or room temperature 25℃ (■), and (D) stability of particle size in the incubation system containing FBS at 37℃ (n=3)

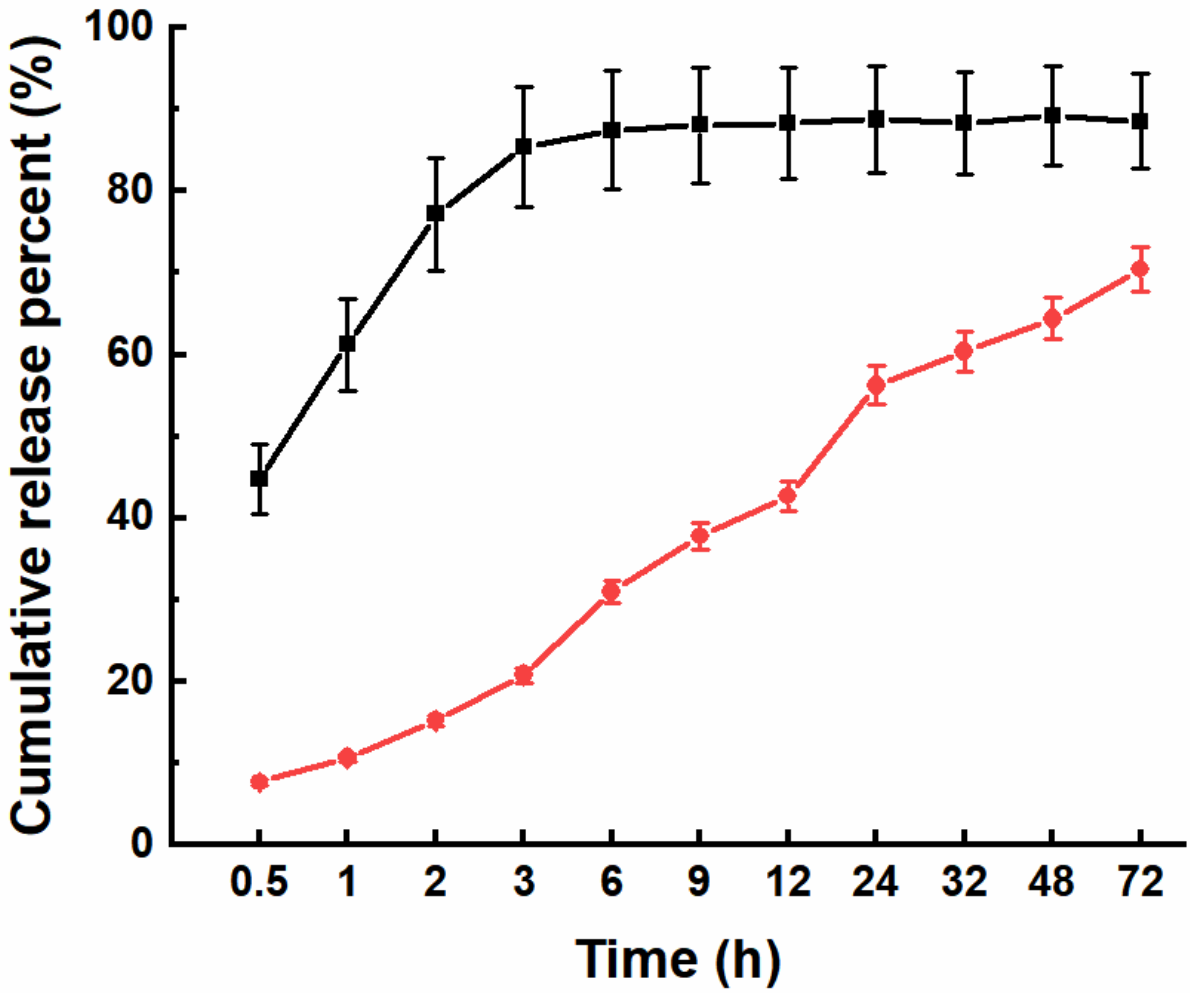

Figure 5

The in vitro release profiles of DOX (■) and SAA (●) from CPMSD in PBS (pH 7.4) at 37°C (n=3)

Figure 6

Evaluation of anticancer characteristics against *in vitro* proliferation of MCF-7 cells. (A) Dose-response relationship of free DOX (mean ± SD, *n*=6). (B) Comparison of antiproliferative effect of the preparations related with CPMSD at an equivalent final concentration of 230 ng/ml for DOX, and 920 ng/ml for SAA, respectively (mean ± SD, *n*=6; * p 0.05 compared with DOX, # p 0.05 compared with CPMSD). (C) CLSM observation (40× objective) of cellular uptake

Figure 7

Evaluation of anticancer efficacy of various preparations in nude mice bearing human breast cancer MCF-7 cells by relative tumor volume (A), tumor weight (B), and body weight change with time (C). (mean ± SD, n=8; ** for $p < 0.01$ compared with the NC group and ## for $p < 0.01$ compared with DOX group. (NC: normal saline, Cocktail: solution of free DOX and SAA, CPMSD: compound micelles of DOX and SAA, DOX group: free DOX solution. Dosage was 2.5 mg/kg for DOX and 10.0 mg/kg for SAA equivalent)

Figure 8

See image above for figure legend.

Figure 9

Evaluation of cardiotoxic effects in nude mice bearing MCF-7 cancer cells by (A) heart weight index, (B) LDH, CK and cTnT in serum, (C) SOD, MDA in heart tissues (**p<0.01 and *p<0.05, compared with NC, $^{\#\#}p$<0.01 and $^{\#}p$<0.05, compared with CPMSD, $^{\&\&}p$<0.01 and $^{\&}p$<0.05, compared with DOX), and (D) light microscope observation (×400) of pathological change in mice left ventricles (with the black arrows indicating representative morphological changes such as cell necrosis, superficial cytoplasm and nucleus and transverse structure loss)